

PSGraph: Differentially Private Streaming Graph Synthesis by Considering Temporal Dynamics

Quan Yuan¹ Zhikun Zhang^{1*} Linkang Du² Min Chen³ Mingyang Sun⁴
Yunjun Gao¹ Michael Backes⁵ Shibo He¹ Jiming Chen^{1,6}

¹Zhejiang University ²Xi'an Jiaotong University

³Vrije Universiteit Amsterdam ⁴Peking University

⁵CISPA Helmholtz Center for Information Security

⁶Hangzhou Dianzi University

Abstract—Streaming graphs are ubiquitous in daily life, such as evolving social networks and dynamic communication systems. Due to the sensitive information contained in the graph, directly sharing the streaming graphs poses significant privacy risks. Differential privacy, offering strict theoretical guarantees, has emerged as a standard approach for private graph data synthesis. However, existing methods predominantly focus on static graph publishing, neglecting the intrinsic relationship between adjacent graphs, thereby resulting in limited performance in streaming data publishing scenarios. To address this gap, we propose PSGraph, the first differentially private streaming graph synthesis framework that integrates temporal dynamics. PSGraph adaptively adjusts the privacy budget allocation mechanism by analyzing the variations in the current graph compared to the previous one for conserving the privacy budget. Moreover, PSGraph aggregates information across various timestamps and adopts crucial post-processing techniques to enhance the synthetic streaming graphs. We conduct extensive experiments on four real-world datasets under five commonly used metrics. The experimental results demonstrate the superiority of PSGraph.

1. Introduction

Streaming graphs, composed of a series of continuous graphs, are prevalent in real-world systems, such as dynamic social networks [41], ongoing communication topologies [27], etc. Analyzing these streaming graphs allows systems to offer more valuable services, including hotspot tracking [55], behavior analysis [39], and advertising recommendations [54]. For example, event propagation can be predicted through the analysis of dynamic social networks [26]. However, these graph data often contain personal private information, such as user relationships and purchase records, which hinders the sharing of these graphs.

Differential privacy (DP) [13], regarded as the gold standard in the privacy community, has been applied to

safeguard the privacy of graph data [40]. The core idea of DP is to ensure that the presence or absence of a single node or edge has a limited impact on the final output. Most previous works on differentially private graph analysis focus on developing specialized methods for specific tasks, such as degree distribution [22] and clustering coefficient [50]. However, these task-specific solutions are not versatile enough to accommodate arbitrary downstream analysis tasks, limiting their applicability.

In this paper, we focus on a more universal and realistic paradigm: publishing synthetic streaming graphs composed of continuously evolving graphs while satisfying DP, thereby enabling various downstream graph analysis tasks. There are several existing studies investigating *static graph synthesis* with DP guarantee [9], [35], [52], [56]. These static graph synthesis methods typically involve encoding the original graph, perturbing the encoded information, and then reconstructing the entire graph or directly perturbing the graph's adjacency matrix. The most straightforward method for *streaming graph synthesis* is to evenly allocate the total privacy budget and independently publish the graph at each timestamp using existing static synthesis methods. However, the edge changes in streaming graphs often exhibit certain dynamic patterns, with changes in adjacent timestamps generally being relatively gentle. The above approach fails to utilize this temporal dynamics between the adjacent consecutive graphs, resulting in a waste of privacy budget and low fidelity of the generated stream data.

Our Proposal. We propose PSGraph, which leverages the temporal dynamics of the streaming graphs across different timestamps for more efficient privacy budget allocation and enhanced utility. The core idea is to adjust the allocation of the privacy budget according to the severity of the streaming graph changes. Considering the characteristics of streaming data, we develop two distinct privacy budget allocation strategies. The appropriate allocation method is selected based on the dynamic changes observed in the streaming graphs between consecutive timestamps. For significant changes, we allocate a portion of the total privacy budget to effectively capture these variations. In contrast, for minor

*. Zhikun Zhang is the corresponding author.

variations, the privacy budget for capturing information can be retained, and more budget is allocated to information perturbation in order to enhance synthetic data utility.

Concretely, to preserve key information while reducing disruption, PSGraph first employs communities as granularity to extract and perturb graph data. Recognizing that the community structure of streaming graphs can undergo subtle or drastic changes at continuous timestamps, which can be captured for better synthetic quality, PSGraph adopts a community judgment mechanism to deal with the variations in the first phase. If changes between adjacent timestamps are small, PSGraph chooses to retain the previous community partition to conserve privacy budget. Conversely, PSGraph tries to re-partition the graph if there are significant variations. During the next phase, PSGraph obtains the noisy node degree information and edge counts between communities. If the community partition of the current timestamp is from the previous timestamp, PSGraph tries to integrate the node information of the two timestamps. Based on the perturbed information, in the last phase, PSGraph reconstructs the entire graph within and between communities using different edge probability formulas. Necessary post-processing is utilized to enhance the fidelity of the generated streaming graphs.

Evaluation. We conduct experiments on four real-world streaming graph datasets to demonstrate the superiority of PSGraph. The experimental results show that PSGraph outperforms other solutions in most cases. For instance, with a privacy budget of 1, PSGraph achieves a 143.5% lower KL divergence in degree distribution compared to the best baseline method on the Cit-HepPh dataset. We further analyze the effect of various components in PSGraph through ablation studies and explore the impact of hyperparameter settings. The related results highlight the crucial role of temporal dynamics in enhancing the performance of PSGraph. For example, when the privacy budget is 2, PSGraph leveraging temporal dynamics achieves an 85.1% higher overlap ratio of eigenvalue nodes on the Reddit dataset compared to PSGraph that ignores this feature (*i.e.*, independently perturbation at each timestamp). In addition, we also evaluate the performance of all methods across different timestamps. We observe that PSGraph almost outperforms other competitors across all timestamps.

Contributions. In summary, the main contributions of the paper are three-fold:

- We propose PSGraph, the first differentially private graph synthesis framework designed for streaming graphs.
- PSGraph employs communities as granularity to extract and perturb information from the original graph, reducing noise injection while preserving critical details. Furthermore, PSGraph leverages temporal dynamics across various timestamps in stream data, introduces a community judgment mechanism to conserve privacy budgets, and incorporates post-processing to enhance the utility of synthesized streaming graphs.
- We conduct extensive experiments on multiple datasets and metrics to illustrate the effectiveness of PSGraph.

2. Preliminaries

2.1. Differential Privacy

Differential privacy (DP) [13] was originated for the data privacy protection scenarios, where a trusted data curator collects data from individual users, perturbs the aggregated results, and then publishes them. Intuitively, DP guarantees that any single sample from the dataset has a limited impact on the output. Formally, DP can be defined as follows:

Definition 1 (ϵ -Differential Privacy). *An algorithm \mathcal{A} satisfies ϵ -differential privacy (ϵ -DP), where $\epsilon > 0$, if and only if for any two neighboring datasets D and D' , and for any possible output set O , we have*

$$\Pr[\mathcal{A}(D) \in O] \leq e^\epsilon \Pr[\mathcal{A}(D') \in O].$$

Here, we consider two datasets D and D' to be *neighbors*, denoted as $D \simeq D'$, if and only if $D = D' + r$ or $D' = D + r$, where $D + r$ represents the dataset resulted from adding the record r to the dataset D .

Laplace Mechanism. This mechanism satisfies the DP requirements by adding random Laplace noise to the aggregated results. The magnitude of the added noise depends on GS_f , *i.e.*, the *global sensitivity*, defined as,

$$GS_f = \max_{D \simeq D'} \|f(D) - f(D')\|_1,$$

where f is the aggregation function. When f outputs a scalar, the Laplace mechanism \mathcal{A} can be given below:

$$\mathcal{A}_f(D) = f(D) + \text{Lap}\left(\frac{GS_f}{\epsilon}\right),$$

where $\text{Lap}(\beta)$ denotes a random variable sampled from the Laplace distribution $\Pr[\text{Lap}(\beta) = x] = \frac{1}{2\beta} e^{-|x|/\beta}$. When f outputs a vector, \mathcal{A} adds independent samples of $\text{Lap}(\beta)$ to each element of the vector.

Composition Properties of DP. The following composition properties of DP are commonly adopted for building complex differentially private algorithms from simpler sub-routines [15].

- **Sequential Composition.** Combining multiple sub-routines that satisfy differential privacy for $\{\epsilon_1, \dots, \epsilon_k\}$ leads to a mechanism satisfying ϵ -DP for $\epsilon = \sum_i \epsilon_i$.
- **Parallel Composition.** Given k algorithms working on disjoint subsets, each satisfying DP for $\{\epsilon_1, \dots, \epsilon_k\}$, the result satisfies ϵ -DP for $\epsilon = \max\{\epsilon_i\}$.
- **Post-processing.** Given an ϵ -DP algorithm \mathcal{A} , releasing $g(\mathcal{A}(D))$ for any g still satisfies ϵ -DP. In other words, post-processing an output of a differential private algorithm does not result in additional loss of privacy.

2.2. Differentially Private Stream Analysis

To address the privacy concerns in the release of the data stream, the concepts of *event-level* privacy and *user-level* privacy are first proposed [14]. Event-level privacy safeguards a single timestamp within a data stream, which

may not offer sufficient privacy guarantees for an entire data stream. On the other hand, user-level privacy is dedicated to concealing all timestamps in a data stream, providing stronger privacy assurances. However, it is inappropriate for infinite streams, which necessitates an infinite amount of perturbation. To balance privacy protection and data utility, *w-event privacy* is proposed to safeguard arbitrary *w* consecutive timestamps in a stream [25].

We first introduce the notion about *stream prefix* and *neighboring streams*. Let $T = \{D_1, D_2, \dots\}$ represents an infinite series, and $T[i] = D_i$ corresponds to the data at i -th time step. The stream prefix S_t is defined as $T_t = \{D_1, D_2, \dots, D_t\}$, representing the sequence of values up to t -th time step. Based on this, the concept of *w-neighboring* can be given as follows:

Definition 2 (*w-neighboring*). Two stream prefixes T_t and T'_t are *w-neighboring*, if for each pair of $T_t[i]$, $T'_t[i]$ such that $i \in \{1, 2, \dots, t\}$ and $T_t[i] \neq T'_t[i]$, it holds that $T_t[i]$, $T'_t[i]$ are neighboring; and for each $T_t[i_1], T_t[i_2], T'_t[i_1], T'_t[i_2]$ with $i_1 \leq i_2, T_t[i_1] \neq T'_t[i_1]$ and $T_t[i_2] \neq T'_t[i_2]$, it holds that $i_2 - i_1 + 1 \leq w$.

Two stream prefixes are *w-neighboring*, which means all their pairwise unequal values could fit in a window of up to w timestamps.

Definition 3 (*w-event privacy*). An algorithm \mathcal{A} satisfies *w-event ε -DP* (or *w-event privacy*), where $\varepsilon > 0$, if and only if for any two *w-neighboring* stream prefixes T_t and T'_t , and for any possible output set O , we have

$$\Pr[\mathcal{A}(T_t) \in O] \leq e^\varepsilon \Pr[\mathcal{A}(T'_t) \in O].$$

A protection mechanism satisfies *w-event privacy* can provide ε -DP guarantee in any sliding window of size w . If $w = 1$, it degenerates to event-level privacy. When w is set to the length of a finite stream, *w-event privacy* converges to user-level privacy.

2.3. Differentially Private Graph Analysis

Edge-DP [22] provides rigorous theoretical guarantees to protect the privacy of the edges by limiting the impact of any edges in the graph on the output. Specifically, given a graph $G = (V, E)$, its edge neighboring graph $G' = (V', E')$ is originated by adding (or removing) an edge, where V (V') denotes the set of nodes and E (E') denotes the set of edges. According to [22], the system difference $a \oplus b$ is the sets of elements in either set a or set b , but not in both, i.e., $a \oplus b = (a \cup b) \setminus (a \cap b)$. Therefore, the definitions of edge neighboring graph and ε -edge DP are as follows.

Definition 4 (Edge neighboring graph). Given a graph $G = (V, E)$, a graph $G' = (V', E')$ is an *edge neighboring graph* of G if and only if $|V \oplus V'| + |E \oplus E'| = 1$.

Definition 5 (ε -edge differential privacy). An algorithm \mathcal{A} satisfies *ε -edge differential privacy* (*ε -edge DP*), where $\varepsilon >$

0. If and only if for any two edge neighboring graphs G and G' , and for any possible output set O , we have

$$\Pr[\mathcal{A}(G) \in T] \leq e^\varepsilon \Pr[\mathcal{A}(G') \in T].$$

According to the privacy definitions of stream data and graph data, we can further give the concepts of *w-edge neighboring graph* and *w-event edge privacy*.

Definition 6 (*w-edge neighboring graph*). Two streaming graph prefixes G_t and G'_t are *w-edge neighboring*, if for each $G_t[i], G'_t[i]$ such that $i \in \{1, 2, \dots, t\}$ and $G_t[i] \neq G'_t[i]$, it holds that $G_t[i], G'_t[i]$ are edge neighboring graphs; and for each $G_t[i_1], G_t[i_2], G'_t[i_1], G'_t[i_2]$ with $i_1 \leq i_2, G_t[i_1] \neq G'_t[i_1]$ and $G_t[i_2] \neq G'_t[i_2]$, it holds that $i_2 - i_1 + 1 \leq w$.

Definition 7 (*w-event edge privacy*). An algorithm \mathcal{A} satisfies *w-event ε -edge DP* (or *w-event edge privacy*), where $\varepsilon > 0$, if and only if for any two *w-edge neighboring* streaming graph prefixes G_t and G'_t , and for any possible output set O , we have

$$\Pr[\mathcal{A}(G_t) \in O] \leq e^\varepsilon \Pr[\mathcal{A}(G'_t) \in O].$$

w-event edge privacy can achieve edge protection for any continuous w graphs with a total privacy budget of ε in the streaming graphs.

3. Problem Definition and Strawman Solution

3.1. Problem Definition

There are many scenarios in real life that require analysis of continuously changing graph data to provide services, e.g., social networks and transportation networks. Due to privacy concerns, the trusted curator usually publishes synthetic data that satisfies differential privacy instead of directly releasing the original data [60]. The synthetic graph dataset is expected to retain similar properties to the original graph and serve as a secure substitute for the original data. In this paper, we consider an undirected and unweighted graph database \mathcal{G}_{orig} that consists of streaming graph $G_t = (V_t, E_t)$, where V_t is the set of nodes and E_t is the set of edges at timestamp t . The goal is to find a release mechanism \mathcal{R} , which takes inputs from \mathcal{G}_{orig} and outputs a dynamic synthetic graph database \mathcal{G}_{syn} at each t . \mathcal{R} satisfies *w-event edge privacy*. We summarize the frequently used mathematical notations in Table 1.

3.2. Strawman Solution

A straightforward approach to address this streaming graph publishing problem is to evenly distribute the total privacy budget at each timestamp and then utilize existing differentially private synthesis methods for releasing static graphs. These synthesis methods for static graphs typically fall into two categories. The first way involves encoding the original static graph, adding noise to the encoded data to

TABLE 1: Summary of mathematical notations.

Notation	Description
t	Timestamp
G_t	Graph at the timestamp t
ϵ	Privacy budget
w	The window size
N^t	The number of nodes of G_t
m^t	The number of edges of G_t
\mathbb{C}	The set of community partitions
C	The community composed of nodes
D_i	Degree information within the community
D_o	Degree information outside the community
V	Edge count between communities

satisfy DP, and then reconstructing the graph. Another way is to directly perturb the entire adjacency matrix.

However, streaming graph data exhibits dynamic variations where adjacent graphs can show close relationships or undergo significant changes. The current graph may experience minor changes from the previous timestamp, involving only a few edges, or it may undergo significant variations involving a large number of edges. Accurately capturing these dynamic changes while satisfying the DP guarantee presents considerable challenges for existing methods. First, existing static methods are optimized for single graph data publishing problems, thus struggling to effectively handle such dynamics. Moreover, the release of streaming data imposes demands on real-time performance, necessitating high efficiency for the designed method. Third, in streaming data scenarios, the entire privacy budget needs to be divided for a series of graph data. Thus, it is more challenging to achieve a proper balance between privacy protection and data utility.

4. Our Proposal: PSGraph

4.1. Motivation

To address the aforementioned challenges, we develop our approach from two perspectives to ensure data utility, *i.e.*, the fidelity of individual graph data and the dynamics of a series of graph data in a data stream. For each individual graph data in the data stream, we want to retain as much information as possible, necessitating careful encoding of graph data. When synthesizing a graph under edge-DP, directly perturbing each edge in the adjacency matrix may introduce excessive noise, whereas compressing the graph into node degrees can lead to significant information loss. According to [56], community is an informative granularity that can reduce noise while preserve key information. Inspired by this, we choose to partition all nodes into communities and perturb the aggregated information. For the dynamics of a series of graph data, we aim to identify and leverage the variations of streaming graphs in privacy-preserving synthesis. We hope to select an appropriate privacy budget allocation strategy according to the extent of variations between adjacent timestamps in order to enhance the utility of the data stream. Based on the above considerations, we design a

streaming graph publishing method, called PSGraph, which rigorously adheres to w -event privacy requirements while ensuring high data utility.

4.2. Overview

As depicted in Figure 1, the workflow of PSGraph mainly consists of three phases: Community determination, information perturbation, and graph reconstruction. The new graphs are continually generated through the three phases, forming streaming graphs. Based on the original graph dataset, the trusted aggregator maintains a synthetic dataset for publishing.

Phase 1: Community Determination. We design a dynamic community determination mechanism to obtain node partitioning for each timestamp. The core idea is to determine the community partitioning strategy based on the differences between the current and previous graphs. If the variations in these graphs are small, we can stick with the previous community divisions, thereby conserving the privacy budget for other phases. Conversely, if there are significant changes over time, we need to re-partition the nodes in the graph and conduct the following phases. The details of Phase 1 can be found in Section 4.3.

Phase 2: Information Perturbation. Based on the community partitioning results from Phase 1, we further encode and perturb three kinds of edge information, *i.e.*, the node’s connections in its community, the node’s connections to other communities, and the connections between different communities. Considering the coherence between the graphs, we choose to integrate the perturbed information from both the current and previous timestamps to enhance the accuracy of the data if the variations between the graphs are not significant. The details of Phase 2 are in Section 4.4.

Phase 3: Graph Reconstruction. Using the perturbed information obtained in the second phase, PSGraph reconstructs the edges both within and between communities according to different probabilistic edge connection formulas. To maintain a more realistic graph distribution, PSGraph performs post-processing on the initially generated graph, ensuring that the total number of edges in the synthetic graph is close to the original graph. The details of Phase 3 are referred to Section 4.5.

The aforementioned three phases form the overall process of PSGraph. Due to space limitations, we defer the complete pseudo-code to Appendix A.

4.3. Community Determination

During the community determination phase, it is crucial to assess the changes between the current and previous graphs. Here, we judge an obvious change between the two graphs by examining the variation in the number of edges. The primary reasons for selecting the number of edges as an indicator are as follows: Firstly, significant variations in community characteristics typically arise from alterations in edges. Secondly, the edge count in a graph tends to be a large value, and its sensitivity is only 1, allowing it to accurately

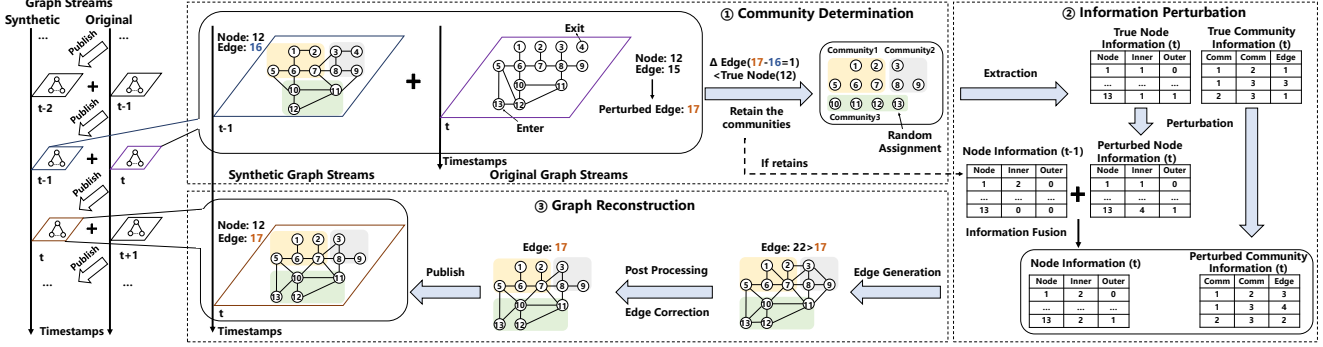


Figure 1: PSGraph overview. PSGraph is composed of three phases: Community determination, information perturbation, and graph reconstruction. In the community determination phase, the difference in edges between the last graph and the current graph is adopted to determine whether to retain the previous community division or community re-partitioning. In the information perturbation phase, node degree information within and across communities, as well as inter-community connections, is extracted and perturbed to satisfy DP. If the current community partition is from the last partition, the final estimated result integrates the perturbed information from both the current and last timestamps. An initial graph is constructed using the edge probability formulas in the graph reconstruction phase. Then, PSGraph utilizes post-processing to adjust the generated graph.

reflect the feature of the original graph under a small privacy budget. Additionally, the number of edges can assist the graph reconstruction process detailed in Section 4.5.

Algorithm 1 outlines the basic process of community determination. We first apply the Laplace mechanism at each moment to obtain the number of perturbed edges for subsequent judgment and processing. The privacy budget consumed in this step is ε_e , with sensitivity $\Delta f_e = 1$. When synthesizing the first graph in the streaming data, historical information is unavailable, necessitating the allocation of a privacy budget for community partitioning. Here, we utilize the community division method proposed in [56] to achieve differentially private community partitioning (i.e., *Comm_div*). The general idea is to first randomly merge the nodes of the original graph into several super-nodes. Subsequently, it employs the Louvain approach [5] to partition the perturbed super-node graph into communities. Finally, by considering the number of edges of nodes to various communities, the exponent mechanism [34] is applied to fine-tune the community assignments of individual nodes. Following the aforementioned operations, we can obtain the community partitioning result \mathbb{C}_D for the initial graph.

When $t > 1$, the previous graph information can aid in determining the community structure of the current graph. First, the change in edge count δ_e between the two graphs can be estimated based on the number of perturbed edges in the previous and current steps. According to [30], many graphs densify over time, with the number of edges growing super-linearly in the number of nodes. Thus, we choose the number of nodes in the graph as a basis for judging whether there has been a significant difference between the communities of the two graphs. If δ_e exceeds the number of nodes N^t , indicating a significant alteration in the graph's community structure, conducting a new node partition is necessary. This process is similar to the community partitioning method adopted at the first timestamp.

On the other hand, if the variation in the number of edges

Algorithm 1: Community Determination

Input: Current timestamp t , original graph G_t , privacy budget $\varepsilon_e^t, \varepsilon_c^t$, the number of nodes of current graph N^t , the number of perturbed edges of last graph m_{pert}^{t-1} (if $t > 1$), the last community division \mathbb{C}_L (if $t > 1$)

Output: the number of perturbed edge m_{pert}^t , community division $\mathbb{C}_D = \{C_1^t, C_2^t, \dots\}$

- 1 Obtain m_{pert}^t by perturbing the true value m^t
- 2 $m_{pert}^t \leftarrow m^t + \text{Laplace}(\varepsilon_e^t, \Delta f_e)$
- 3 **if** $t = 1$ **then**
- 4 Perform community partitioning on nodes of G_t
- 5 $\mathbb{C}_D \leftarrow \text{Comm_div}(G_t, \varepsilon_c^t)$
- 6 **else**
- 7 $\delta_e = |m_{pert}^t - m_{pert}^{t-1}|$
- 8 // Community judgment
- 9 **if** $\delta_e > N^t$ **then**
- 10 $\mathbb{C}_D \leftarrow \text{Comm_div}(G_t, \varepsilon_c^t)$
- 11 **else**
- 12 $\mathbb{C}_D \leftarrow \mathbb{C}_L$
- 13 Update \mathbb{C}_D by randomly assigning newly added nodes at time t to existing communities.

is small, the community partitioning from the previous step can be reused. In this case, the surplus privacy budget ε_e^t is reserved for the subsequent phase of information perturbation, which helps to reduce the perturbation intensity.

4.4. Information Perturbation

Based on the community partition obtained in the first phase \mathbb{C}_D , information extraction and perturbation can be strategically conducted from both node-level and

community-level perspectives, thereby achieving a good balance between privacy and utility. Algorithm 2 illustrates the process of the information perturbation phase.

The first step is to extract information from nodes and communities. For each node, we count the number of edges within its community D_i^t and the number of edges connecting to other communities D_o^t separately. On one side, this operation effectively aggregates the connection information of nodes, avoiding excessive perturbation. On the other side, gathering information under community granularity helps preserve nodes' characteristics. Considering that the number of communities is usually large, to accurately capture edge information across various communities under high privacy protection requirements, we also calculate the total number of external edges between any two communities V^t .

In the second step, PSGraph perturbs the extracted information in the first step, *i.e.*, the node degrees and edge counts between communities. The Laplace mechanism is applied to satisfy differential privacy. Since an edge can influence two nodes simultaneously, the sensitivity of degree information Δf_d is 2. The sensitivity of edge count between communities Δf_v is 1. In this paper, we set $\varepsilon_{i1}^t = \varepsilon_{i2}^t = 0.5\varepsilon_i^t$ to achieve a balance between degree information and edge count. Furthermore, the degree information outside the community and the edge count between different communities overlap, necessitating the consumption of separate privacy budgets, ε_{i1}^t and ε_{i2}^t , respectively. Conversely, degree information for nodes within the community does not overlap with the above parts. Therefore, the degree of nodes within the community can be protected using the privacy budget of $\varepsilon_i^t = \varepsilon_{i1}^t + \varepsilon_{i2}^t$.

In practice, the perturbed values of node's degree or edge count may be negative, which conflicts with their definitions. To address this issue, we employ the NormSub [48] method to process the perturbed values. Given the estimated edge count vector \tilde{V}^t , we hope to find an optimal integer δ^* :

$$\delta^* = \arg \min_{\delta} \left| \sum_{a \in \mathbb{C}_{\mathbb{D}}} \max(\tilde{V}_a^t + \delta, 0) - \sum_{a \in \mathbb{C}_{\mathbb{D}}} \tilde{V}_a^t \right|.$$

Then, we update the value of \tilde{V}_a^t to $\max(\tilde{V}_a^t + \delta^*, 0)$. Through the consistency processing, we ensure that the edge counts between communities adhere to non-negative constraints. Similarly, we apply NormSub to handle estimated degree vectors both within and outside the communities.

In real-world scenarios, many streaming graphs demonstrate relatively consistent features between successive timestamps, which can aid in obtaining more accurate information. Here, we assess the necessity of utilizing information from the last timestamp based on the sources of community partitioning. If current community partitioning $\mathbb{C}_{\mathbb{D}}$ builds upon previous partitioning results $\mathbb{C}_{\mathbb{L}}$, we can integrate information from both steps to achieve a more precise estimate, especially under limited privacy budgets.

In particular, we employ a weighted approach to obtain final degree estimate for overlapping nodes at two timestamps. By taking into account the privacy budget of the two parts, the final degree information can be updated as follows:

Algorithm 2: Information Perturbation

Input: Current timestamp t , Original graph G_t , current community division $\mathbb{C}_{\mathbb{D}}$, privacy budget $\varepsilon_i^t, \varepsilon_{i1}^t, \varepsilon_{i2}^t = \varepsilon_i^t - \varepsilon_{i1}^t$

Output: Noisy degree information within the community \hat{D}_i^t , noisy degree information outside the community \hat{D}_o^t , noisy edge count between various communities \hat{V}^t

```

1 Step 1: Information extraction
2 for node in  $G_t.nodes()$  do
3   Extract the node's degree information  $d_i$  within
   its community, and the node's degree
   information  $d_o$  outside its community
4   Update  $D_i^t$  and  $D_o^t$  based on  $d_i$  and  $d_o$ 
5 for  $C_a, C_b (a \neq b)$  in  $\mathbb{C}_{\mathbb{D}}$  do
6   Extract the number of edges  $v_{a,b}$  between
   community  $C_a$  and  $C_b$ 
7   Update  $V^t$  based on  $v_{a,b}$ 
8 Step 2: Noise injection
9 // The degree information outside the community
   and the edge count between various communities
   consume the total privacy budget  $\varepsilon_i^t$ 
10  $\tilde{D}_i^t \leftarrow D_i^t + Laplace(\varepsilon_i^t, \Delta f_d)$ 
11  $\tilde{D}_o^t \leftarrow D_o^t + Laplace(\varepsilon_{i1}^t, \Delta f_d)$ 
12  $\tilde{V}^t \leftarrow V^t + Laplace(\varepsilon_{i2}^t, \Delta f_v)$ 
13 Step 3: Consistency processing
14  $\bar{D}_i^t \leftarrow NormSub(\tilde{D}_i^t)$ ,  $\bar{D}_o^t \leftarrow NormSub(\tilde{D}_o^t)$ ,
    $\bar{V}^t \leftarrow NormSub(\tilde{V}^t)$ 
15 Step 4: Information fusion
16 if  $\mathbb{C}_{\mathbb{D}}$  is based on  $\mathbb{C}_{\mathbb{L}}$  then
17    $\hat{D}_i^t \leftarrow Combine(\bar{D}_i^t, \hat{D}_i^{t-1})$ 
18    $\hat{D}_o^t \leftarrow Combine(\bar{D}_o^t, \hat{D}_o^{t-1})$ 
19 else
20    $\hat{D}_i^t \leftarrow \bar{D}_i^t$ 
21    $\hat{D}_o^t \leftarrow \bar{D}_o^t$ 

```

$$\begin{aligned} \hat{D}_i^t &= \alpha_1 \bar{D}_i^t + (1 - \alpha_1) \hat{D}_i^{t-1}, \\ \hat{D}_o^t &= \alpha_2 \bar{D}_o^t + (1 - \alpha_2) \hat{D}_o^{t-1}, \end{aligned}$$

where $\alpha_1 = \frac{\varepsilon_i^t}{\varepsilon_i^t + \varepsilon_{i1}^{t-1}}$ and $\alpha_2 = \frac{\varepsilon_{i1}^t}{\varepsilon_{i1}^t + \varepsilon_{i1}^{t-1}}$. The higher the privacy budget, the greater the fidelity of information, and therefore, the corresponding weight should be higher. By considering the privacy budget and node degree information across adjacent timestamps, we can better capture the dynamic features in the streaming graphs.

4.5. Graph Reconstruction

In this phase, we need to reconstruct the whole graph based on the perturbed degree information and edge count between communities. Due to the different perturbation strategies of the extracted nodes within and outside the community, it is improper to adopt the same reconstruction method for these two types of edges. Therefore, we

initially utilize distinct reconstruction methods for intra-community and inter-community connections and then apply post-processing to the generated graph. The detailed process is shown in [Algorithm 3](#).

For the intra-community edges, on the basis of perturbed \hat{D}_i^t , we utilize the CL model [2] to generate the subgraph in each community, which can effectively recover the degree information and satisfy the power-law distribution. Assuming that \hat{d} is the perturbed degree sequence within the community C_a , the connection probability between node x and node y within the community C_a is as follows.

$$p_{x \in C_a, y \in C_a} = \frac{\hat{d}_a^x \cdot \hat{d}_a^y}{\sum_{z \in C_a} \hat{d}_a^z}, \quad (1)$$

where \hat{d}_a^x and \hat{d}_a^y stand for the degrees of node x and y within the community C_a , and the denominator is the sum of node degree in C_a .

For the connections between communities, the two types of information extracted can be effectively combined, namely the degree information of each node outside the community \hat{D}_o^t and the number of connections between communities \hat{V}^t . Assuming node x belongs to the community C_a and node y belongs to the community C_b , our objective is to estimate the probability of connection between nodes x and y . \hat{h} represents the perturbed degree sequence outside the community, and \hat{v} represents the perturbed edge count between communities. Firstly, the expected number of edges from the node to other communities can be calculated. For instance, the expected number of edges \hat{e}_x^b from node x to community C_b is:

$$\hat{e}_x^b = \hat{h}_x \cdot \frac{\hat{v}_{a,b}}{\sum_{g \in C_D} \hat{v}_{a,g}}, \quad (2)$$

where \hat{h}_x is the perturbed degree information outside the community C_a for node x , $\hat{v}_{a,b}$ is the perturbed edge count between community C_a and community C_b , the denominator is the sum of the number of edges between community C_a and other communities. Similarly, we can obtain the expected number of edges \hat{e}_y^a from node y to community C_a . Based on the expected number of edges mentioned above, we further estimate the probability of connected edges between nodes x and y :

$$p_{x \in C_a, y \in C_b} = \frac{\hat{e}_x^b \cdot \hat{e}_y^a}{\sum_{z \in C_b} \hat{e}_z^a}, \quad (3)$$

where the denominator is the sum of the expected number of edges from all nodes in the community C_b to the community C_a . Note that the denominator can also be the sum of the expected number of edges from all nodes in the community C_a to the community C_b .

Using the formula mentioned above, we can initial the connections both within and between communities. However, the graph generated may not align perfectly with the original expected information, particularly in cases with significant noise perturbation. Therefore, we aim to enhance the utility of the generated graph by integrating multiple

previously available expected information (*i.e.*, the perturbed total number of edges and the degree information of nodes) for post-processing. We try to ensure that the number of edges and the degree sequence of nodes in the generated graph are as close to the original information as possible.

Firstly, we can obtain the degree information of nodes within and outside the community (*i.e.*, H_i^t and H_o^t) and the total number of generated edges m_g^t . Additionally, for all nodes, we can compute the disparity (*i.e.* ΔM_i^t and ΔM_o^t) between the degree information (*i.e.*, \hat{D}_i^t and \hat{D}_o^t) from the information perturbation phase and the generated degree information (*i.e.*, H_i^t and H_o^t). Furthermore, we merge ΔM_i^t and ΔM_o^t into a unified set (*i.e.*, ΔM^t) for subsequent iterations. Then, we calculate the difference Δm between the perturbed total number of edges m_{pert}^t and the total number of edges m_g^t in the generated graph G_s^t , which can guide the termination criteria for post-processing. If Δm is greater than 0, it indicates that the perturbed number of edges exceeds the total number of edges in the generated graph, necessitating the addition of several edges to G_s^t . Conversely, if Δm is less than 0, it signifies that some edges need to be removed from the generated graph G_s^t . Next, we illustrate the edge processing steps for $\Delta m > 0$. We begin by sorting all relevant nodes in descending order based on ΔM^t . A higher order indicates a larger difference, implying that more edges need to be added to G_s^t . Note that there are a total of $2N^t$ nodes in the set ΔM^t , as it contains both ΔM_i^t and ΔM_o^t . We iterate through the sorted nodes. In each iteration, we compute the estimated degree information and compare it with the degree information of the generated graph to determine the number of edges m_u that need to be added to node u . We then randomly add m_u edges to the set of candidate nodes that have not yet been connected. Subsequently, we tally the estimated number of edges and the total number of edges in the generated graph and calculate the difference between them Δm_1 . If $\Delta m_1 \leq 0$, the total number of edges in the generated graph is approaching the estimated number of edges, prompting the termination of the loop. Through this post-processing operation, we effectively adjust the degree information of the generated graph and align its density with that of the original graph.

4.6. Algorithm Analysis

Privacy Budget Analysis. Recalling [Figure 1](#), in each timestamp, PSGraph includes three phases, *i.e.*, community determination, information perturbation, and graph reconstruction. The community determination phase obtains the number of perturbed edges and finishes the community division, which consume privacy budgets of ε_e^t and ε_c^t respectively. The privacy budget consumed by the information perturbation phase is ε_i^t . The phase of graph reconstruction does not touch the true data, *i.e.*, without consuming any privacy budget. Therefore, the privacy budget for a single timestamp is $\varepsilon_s = \varepsilon_e^t + \varepsilon_c^t + \varepsilon_i^t$, and the total privacy budget in w timestamps is $\varepsilon = w \cdot \varepsilon_s$. We can obtain the following

Algorithm 3: Graph Reconstruction

Input: Null graph G_N^t , community division \mathbb{C}_D , noisy degree information within the community \hat{D}_i^t , noisy degree information outside the community \hat{D}_o^t , noisy edge count between various communities \hat{V}^t , the number of perturbed edges m_{pert}^t

Output: Synthetic graph G_s^t

- 1 Initialize G_s^t as G_N^t
 - 2 **Step 1: Intra-community edge generation**
 - 3 **for** C_a **in** \mathbb{C}_D **do**
 - 4 Generate subgraph S_a^t based on $\hat{D}_{i,a}^t$ and Equation 1
 - 5 Update G_s^t by S_a^t
 - 6 **Step 2: Inter-community edge generation**
 - 7 **for** $C_a, C_b (a \neq b)$ **in** \mathbb{C}_D **do**
 - 8 Generate subgraph $S_{a,b}^t$ based on $\hat{V}_{a,b}^t$, Equation 2 and Equation 3
 - 9 Update G_s^t by $S_{a,b}^t$
 - 10 **Step 3: Edge post-processing**
 - 11 **For** the generated graph G_s^t , calculate the degree information of nodes within the community H_i^t and outside the community H_o^t , and the total number of generated edges m_g^t
 - 12 $\Delta M_i^t \leftarrow \hat{D}_i^t - H_i^t$, $\Delta M_o^t \leftarrow \hat{D}_o^t - H_o^t$
 - 13 $\Delta M^t \leftarrow \{\Delta M_i^t, \Delta M_o^t\}$
 - 14 Calculate the difference between the estimated number of edges and generated number of edges
 - 15 $\Delta m \leftarrow m_{pert}^t - m_g^t$
 - 16 **if** $\Delta m > 0$ (or $\Delta m < 0$) **then**
 - 17 Sort ΔM^t in descending (or ascending) order
 - 18 **for** *node* u **in** sorted $G_s^t.nodes()$ **do**
 - 19 Calculate the number of edges m_u to be added (or removed) for node u
 - 20 Update G_s^t by randomly adding (or removing) m_u edges from the candidate set
 - 21 Calculate the difference Δm_1 between m_{pert}^t and the total number of edges in current G_s^t
 - 22 **if** $\Delta m_1 \leq 0$ (or $\Delta m_1 \geq 0$) **then**
 - 23 | break
 - 24 Obtain the final synthetic graph G_s^t
-

theorem, and the proof is deferred to Appendix B due to the space limitation.

Theorem 1. PSGraph satisfies w -event ε -edge DP, where $\varepsilon = w \cdot \varepsilon_s$ and $\varepsilon_s = \varepsilon_e^t + \varepsilon_c^t + \varepsilon_i^t$.

Complexity Analysis. We compare the time complexity and the space complexity of various methods. PrivHRG has the highest time complexity while DER has the highest space complexity. The corresponding analysis is in Appendix C.

TABLE 2: Dataset Statistics.

Dataset	Nodes	Edges	Timestamps	Type
As-733 [29]	7,473	22,705	147	Communication
As-caida [29]	31,092	97,164	25	Communication
Cit-HepPh [30]	12,905	764,525	36	Citation
Reddit [28]	34,191	125,162	24	Hyperlink

5. Evaluation

In Section 5.2, we first conduct an end-to-end experiment to illustrate the effectiveness of PSGraph compared to existing state-of-the-art methods for static graph publishing. The baselines are extended to stream scenarios in the same way, which is introduced in Section 3.2. Then, we perform ablation experiments to explore the influence of each component of PSGraph. Next, we verify the impact of the parameter setting of PSGraph. We also provide the performance of various methods at each timestamp.

5.1. Experimental Setup

Datasets. We evaluate the performance of different methods on four real-world datasets. Table 2 provides the total number of nodes and edges from all timestamps of the datasets.

Metrics. Following previous works [35], [37], [56], we evaluate the quality of the synthetic streaming graphs from five different aspects: Eigenvalue nodes, degree distribution, assortativity coefficient, density, clustering coefficient. For the eigenvalue nodes, we compare the overlap ratio of the top 1% most influential nodes. For the degree distribution, we adopt the KL divergence to measure the difference. For the last three metrics, we calculate their relative errors (REs).

Competitors. To our knowledge, there are no other differential privacy synthesis approaches optimized for streaming graphs, and we adopt existing differential privacy synthesis methods for the static graph as the baselines. Specifically, we evenly allocate the total privacy budget across each timestamp. Subsequently, we perturb the original graph individually using these differential privacy synthesis methods for the static graph. The baselines include PrivHRG [52], DER [9], TmF [35], LDPGen [37], and PrivGraph [56]. To ensure a fair comparison, we adopt the recommended parameters from the original papers.

Experimental Settings. For PSGraph, we set the window size $w = 5$, and set the threshold parameter for whether to re-partition the communities to N^t (the number of nodes) in the community determination phase.

Implementation. We explore the performance of various methods with a total privacy budget ε ranging from 0.5 to 4.0. All experiments are implemented on a server with AMD EPYC 7402 24-Core processor and 512GB memory. For each metric, we compute the mean value across all timestamps as a single experimental result. Then, we repeat the experiment 10 times for each setting and report the mean and the standard variance.

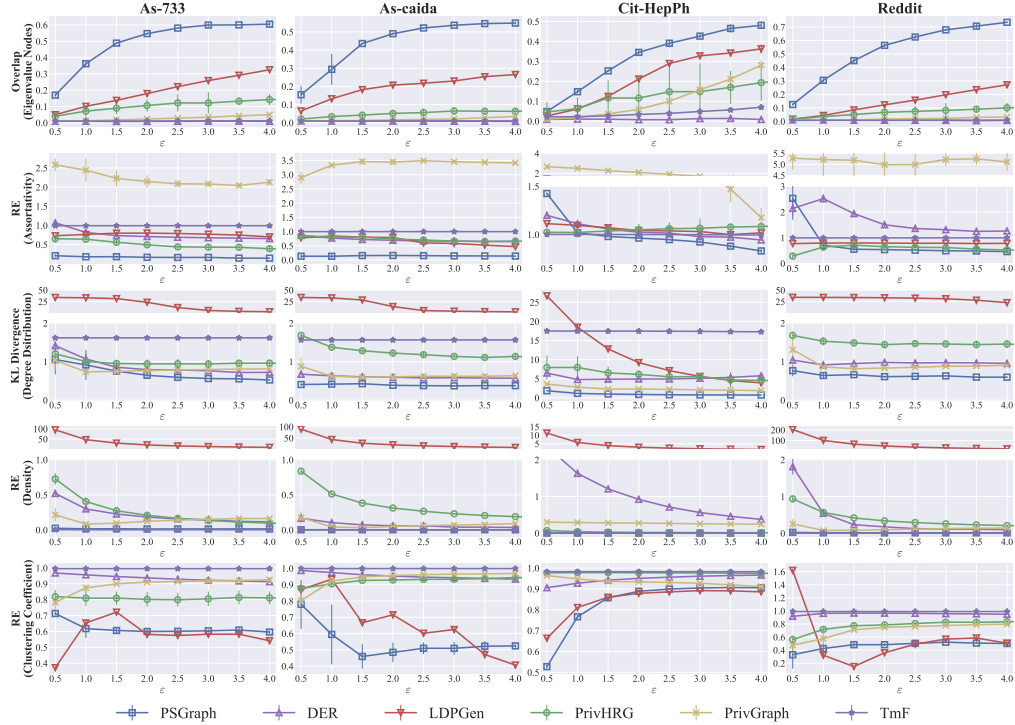


Figure 2: End-to-end comparison of different methods. The columns represent the used datasets, and the rows stand for different metrics. In each plot, the x -axis denotes the privacy budget ϵ , and the y -axis denotes the performance. For the first row, higher is better. For the last four rows, lower is better.

5.2. End-to-End Evaluation

In the section, we perform an end-to-end evaluation of PSGraph and the baselines on five metrics. Figure 2 illustrates the experimental results on four different datasets. **Results on Eigenvalue Nodes.** The first row of Figure 2 shows the overlap of nodes in the top 1% eigenvalues between the original and generated graphs on four datasets, where a higher value stands for higher accuracy. We can obtain the following observations from the results. 1) PSGraph outperforms other methods across all datasets. By obtaining perturbation degree information both within and outside the community, PSGraph effectively preserves the characteristics of influential nodes. Moreover, PSGraph fully leverages streaming data attributes, leading to a more judicious allocation of privacy budget and a higher overlap of feature nodes. 2) LDPGen and PrivHRG perform better than other baseline methods because they incorporate the probability of node connections during their design process, which aids in recovering eigenvalue nodes. 3) PrivGraph demonstrates better performance on the Cit-HepPh dataset compared to others. This is partly due to the dataset’s higher density and more pronounced community clustering, which enhance PrivGraph’s effect. In addition, the small privacy budget allocated per time step adversely affects the performance of PrivGraph. 4) TmF and DER exhibit the poorest performance. The designs of these two methods involve random edge assignments within specific regions,

which are less conducive to preserving eigenvalue nodes.

Results on Assortativity Coefficient. The second row depicts the RE of assortativity coefficients between original and synthetic streaming graphs. We obtain the following key observations. 1) PSGraph outperforms other methods in most cases, especially with higher privacy budgets. This superiority stems from PSGraph’s effective preservation of node features by leveraging the degree information of nodes both within and outside communities and accurately capturing dynamic variations. For the Cit-HepPh dataset, which is a dense network of edges, lower privacy budgets lead to greater disruption of real edges, resulting in higher errors in assortativity coefficients. For the Reddit dataset, the amplitude of this metric is small, resulting in higher relative errors under significant disturbances. 2) PrivGraph shows the weakest performance overall. The reason is that PrivGraph only focuses on protecting the connections between nodes within the community, ignoring the connections between communities, which affects the final recovery. 3) TmF exhibits a RE close to 1 across all datasets due to its random edge assignment approach, lacking node information protection. This randomness leads to higher errors under low privacy budgets. 4) Other mechanisms include PrivHRG, LDPGen, and DER do not consistently perform well on all datasets but show efficacy on specific datasets. Although these methods take into account node connectivity in their designs, their applicability across diverse datasets remains limited.

Results on Degree Distribution. We explore the performance of various methods on the nodes’ degree distribution. We can obtain the following observations from the third row of Figure 2. 1) PSGraph exhibits significantly lower KL divergence across various datasets compared to other methods. This superiority can be attributed to the extraction of node degree information. Furthermore, through information fusion and effective post-processing, PSGraph achieves a high degree of similarity in nodes’ degree distribution between the original and generated graphs. 2) PrivGraph also demonstrates relatively low KL divergence across different datasets. This is due to PrivGraph’s focus on extracting edge information within communities, which aids in preserving the degree distribution of the original graph. 3) DER performs well in degree distribution relative to other baseline methods, except for the Cit-HepPh dataset. The denser connections and higher-degree nodes in the Cit-HepPh dataset make it more susceptible to the random edge assignment of DER, potentially disrupting original node characteristics. 4) PrivHRG and TmF perform less favorably on this metric compared to most other methods, as their designs do not prioritize nodes’ degree preservation. 5) LDPGen exhibits particularly high KL divergence because significant perturbations under small privacy budgets can lead to a substantial increase in edge counts compared to the original graph. This discrepancy significantly impacts the node degree distribution of the generated graph.

Results on Density. The fourth row shows the RE of each method in density, yielding the following observations: 1) PSGraph and TmF excel in density metric, achieving errors close to zero. Both methods perturb the true edge count from the original graph and utilize it as a crucial constraint in their graph synthesis process. 2) PrivGraph also demonstrates relatively small density errors. By protecting the edge counts within and between communities, PrivGraph maintains a density close to that of the original graph. 3) PrivHRG outperforms DER on the Cit-HepPh dataset but performs less effectively on the other three datasets. This disparity is primarily due to the dense edge structure of the Cit-HepPh dataset compared to the sparse edges in others. DER tends to disrupt the original graph’s characteristics more severely under denser edge conditions. 4) LDPGen shows the poorest performance in density. This is because it generates a high number of edges, particularly under low privacy budgets, resulting in a significantly higher density in the synthetic graph compared to the original graph.

Results on Clustering Coefficient. The last row of Figure 2 evaluates the performance of all methods on clustering coefficients, leading to the following observations: 1) PSGraph and LDPGen demonstrate superior performance compared to other methods. PSGraph effectively captures edge information within and between communities, employing meticulous post-processing to enhance the fidelity of the synthesized graph, thereby achieving better clustering coefficient performance. LDPGen utilizes k -means clustering for node grouping, which aids in preserving true clustering coefficients. It’s noteworthy that a larger privacy budget does not mean that the RE of the clustering coef-

ficients is smaller for all datasets. This trend is influenced by dataset characteristics. As-caida and Cit-HepPh datasets exhibit higher clustering coefficients, with the latter being denser. Consequently, the performance trends of LDPGen and PSGraph are relatively consistent in these datasets but diverge in others. The clustering coefficients of the other two datasets are relatively small, so the variations in LDPGen on these two datasets are more drastic. 2) The overall performance of PrivGraph and PrivHRG is better than other baselines. The node’s community partitioning of PrivGraph and the node’s probabilistic connectivity design of PrivHRG contribute to the restoration of true clustering coefficients. 3) DER performs only better than TmF. They do not fully consider the connection conditions between different nodes. TmF randomly allocates edges across the entire adjacency matrix, while DER allocates edges within a certain region. **Takeaways.** In general, the performance of PSGraph is better than other baselines in most cases. Based on the analysis and results, we can obtain the following conclusions.

- PSGraph partitions nodes into communities, perturbs degree information within and between communities, and employs essential post-processing during reconstruction, which effectively preserves assortativity coefficients, density, and clustering coefficients of the real graph.
- PSGraph dynamically evaluates variations in the streaming graphs to decide whether to re-partition communities, integrating information across different timestamps when changes are small. This approach significantly enhances the overlap ratio of eigenvalue nodes and reduces the KL divergence in degree distribution.
- LDPGen utilizes k -means clustering to partition nodes, achieving good performance in clustering coefficients and eigenvalue nodes. PrivGraph focuses on extracting intra-community node edges, thereby achieving a low KL divergence of degree distribution. TmF reconstructs graphs based on the number of perturbed edges, maintaining a density close to that of the original graph. DER groups similar nodes and randomly assigns edges within specific regions, which performs better in the graphs with sparse edges. PrivHRG considers edge connection probabilities between different nodes, resulting in an outstanding performance in terms of assortativity coefficients.

5.3. Ablation Study

5.3.1. Impact of the Community Judgment. Recalling Section 4.3, in the community determination phase, PSGraph assesses whether there has been a significant change in the current graph compared to the previous time. If the change is small, the previously partitioned community remains unchanged; otherwise, the community undergoes re-partitioning. In this section, we validate the effectiveness of the community judgment. Specifically, during the phase of community determination, we perform re-partitioning each time (called PSGraph-R1) and keep the other procedures unchanged. Then, we compare the performance between PSGraph and PSGraph-R1. Figure 3 illustrates the comparison results on two metrics.

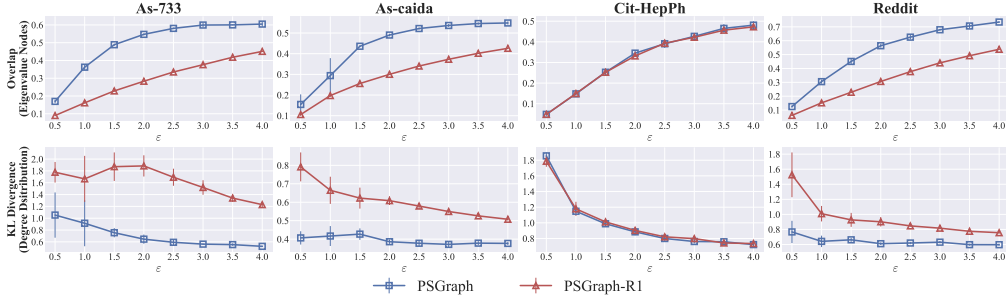


Figure 3: Comparison of PSGraph and PSGraph-R1. The columns represent the used datasets, and the rows stand for different metrics. In each plot, the x -axis denotes the privacy budget ϵ , and the y -axis denotes performance. For the first row, higher is better. For the last row, lower is better.

PSGraph demonstrates significantly superior performance compared to PSGraph-R1 across three datasets, with the exception of the Cit-HepPh dataset. The reason is that the Cit-HepPh dataset exhibits low relationships between various timestamps, unlike the other three datasets, which display high coherence. Consequently, PSGraph-R1 does not yield a pronounced advantage in the Cit-HepPh dataset. In contrast, PSGraph effectively leverages the temporal coherence present in the other datasets. PSGraph retains previous community partitions in moments of small variations, thus conserving the privacy budget for information perturbation in the subsequent phase. This operation ensures the utility of synthetic streaming graphs. From this, we find that whether streaming graphs with drastic changes or streaming graphs with low variations, PSGraph can achieve outstanding performance, which underscores the importance of community judgment. We also provide the comparison results on the other three metrics in [Appendix D.1](#).

5.3.2. Impact of Various Components. Recalling [Section 4.4](#) and [Section 4.5](#), there are two main components in the second and third phases: The information fusion step in the information perturbation phase, and the edge post-processing step in the graph reconstruction phase. We verify the effectiveness of these two steps with four variants called Ablation1, Ablation2, Ablation3, and Ablation4, which are summarized in [Table 3](#).

[Figure 4](#) illustrates the performance of various components on two metrics, and the results on the other three metrics are deferred to [Appendix D.2](#). From [Figure 4](#), Ablation1, excluding both information fusion and post-processing, shows inferior results on both metrics. Ablation2 and Ablation3, incorporating either information fusion or post-processing alone, exhibit a certain improvement compared to Ablation1. Ablation4 achieves the best performance by integrating both information fusion and post-processing, highlighting the pivotal role of these steps. Moreover, due to the drastic changes in the Cit-HepPh dataset, the impact of information fusion is less pronounced on this dataset.

5.4. Parameter Variation

5.4.1. Impact of Window Size. [Figure 5](#) illustrates the performance of different methods across various window

TABLE 3: Details of ablation studies.

Name	Information fusion	Post-processing
Ablation1	×	×
Ablation2	✓	×
Ablation3	×	✓
Ablation4	✓	✓

size w with a privacy budget of 2.5. Due to space constraints, we provide a comparison of the overlap ratio of eigenvalue nodes and the KL divergence of degree distribution. The results highlight the significant advantages of PSGraph over other methods, showcasing the effectiveness of our dynamic community determination mechanism and post-processing steps in allocating privacy budget and enhancing utility. Additionally, as w increases, the overlap of eigenvalue nodes exhibits a declining trend, mainly due to the reduced privacy budget allocated to each timestamp, posing a challenge to graph reconstruction. Nonetheless, PSGraph still maintains great performance compared to other baselines. We also provide the performance of other metrics at various w in [Appendix E.1](#).

5.4.2. Impact of Threshold. Recalling [Section 4.3](#), PSGraph determines whether to re-partition communities based on variations in edge counts between current and previous timestamps. In this section, our aim is to explore the impact of different threshold settings on various metrics. [Figure 6](#) illustrates the REs of eigenvalue node overlap and assortativity coefficients across different privacy budgets, with thresholds ranging from 0.01 times to 100 times the number of nodes. The performance of the other three metrics under various thresholds is provided in [Appendix E.2](#). Our observations are as follows. 1) Datasets show inconsistent performance under the same threshold. For instance, As-733, As caida and Reddit datasets exhibit lower eigenvalue node overlap ratios with smaller thresholds, whereas the Cit-HepPh dataset shows higher overlap ratios under similar conditions. This divergence stems from Cit-HepPh’s more pronounced changes and lower relationships between adjacent timestamps compared to the other datasets. 2) The same metric on a single dataset demonstrates varying trends with different privacy budgets. For example, when $\epsilon = 1.5$, the RE of assortativity coefficient in the As-733 dataset decreases steadily with increasing threshold, while when

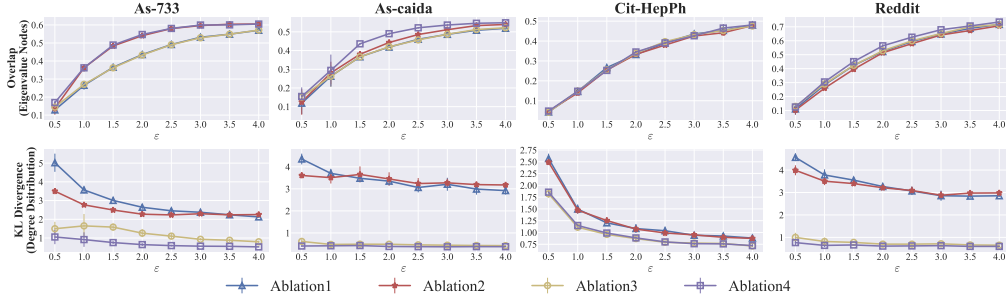


Figure 4: Effectiveness of various ablation components. Ablation1 represents PSGraph without information fusion and post-processing, Ablation2 represents PSGraph without post-processing, Ablation3 represents PSGraph without information fusion, and Ablation4 represents PSGraph. The columns represent the datasets, and the rows stand for different metrics. In each plot, the x -axis denotes the privacy budget ϵ and the y -axis denotes performance. For the first row, higher is better. For the last row, lower is better.

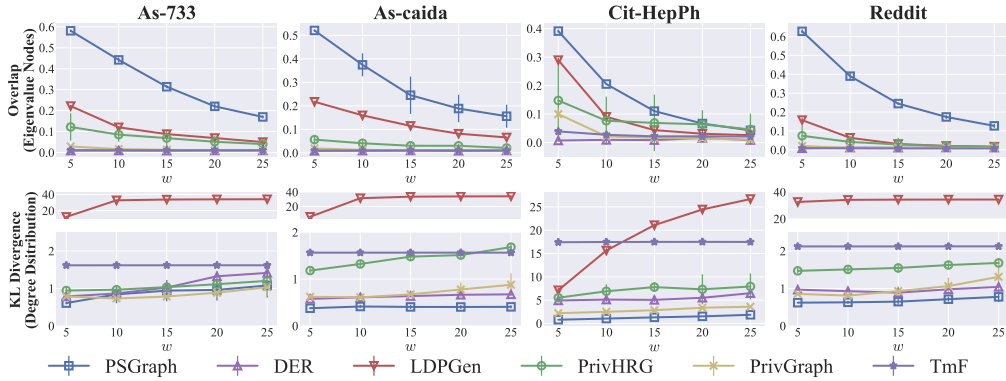


Figure 5: Impact of window size. Different columns stand for different datasets, and different rows stand for different metrics. In each plot, the x -axis denotes the number of window size w and the y -axis denotes performance. For the first row, higher is better. For the last row, lower is better.

$\epsilon = 3.5$, the RE shows an increasing trend with higher thresholds. 3) Under the same dataset and privacy budget, different metrics exhibit distinct trends. For instance, with a privacy budget of 3.5 on the As-733 dataset, small thresholds yield low eigenvalue node overlap ratios and small REs in assortativity coefficient.

Based on these results, we find no single threshold that satisfies all privacy budgets, metrics, and datasets. Overall, PSGraph consistently maintains competitive quality when using the number of nodes as the threshold. Therefore, this criterion is applied uniformly throughout our experiment.

5.5. Detailed Analysis

To further investigate the performance of different methods, we present the overlap ratios of eigenvalue nodes and the REs of the assortativity coefficient at different timestamps on the As-733 dataset when the privacy budget is 2.5 in Figure 7. Notably, PSGraph consistently outperforms other methods across nearly all timestamps. This highlights the critical role played by the community determination mechanism, temporal information utilization, and post-processing steps of PSGraph in preserving the intrinsic characteristics of streaming graphs.

6. Related Work

6.1. Differentially Private Stream Release

Differential privacy has been widely employed in data streaming scenarios where data is continuously published. The privacy notion in stream release mainly includes event-level, user-level, and w -event privacy.

Event-level Privacy. It is utilized to protect individual timestamps [7], [11], [14], [36], [47]. Chen *et al.* [11] employ a perturb-group-smooth architecture to answer multiple stream queries. Perrier *et al.* [36] observe that stream data often concentrates below a threshold significantly lower than the upper bound, devising a method based on the smooth sensitivity mechanism to identify this threshold. Wang *et al.* [47] tackle the issue of unbounded maximum values in real-value data stream publishing using a threshold estimation mechanism. This framework is applicable to both centralized and local settings for event-level privacy.

User-level Privacy. Compared to event-level DP, which protects against changes in individual events, user-level privacy aims to hide all events of any user [1], [12], [16], [17], [31]. Fan *et al.* [17] propose a framework that releases perturbed statistics at sampled timestamps and utilizes the

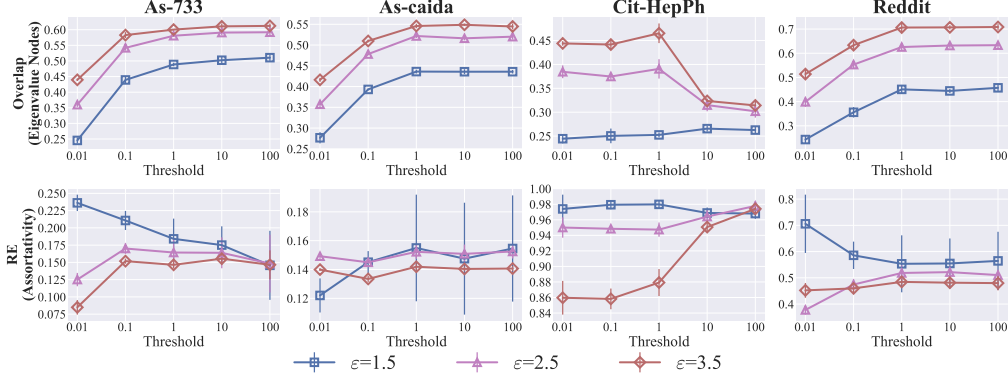


Figure 6: Impact of threshold. Different columns stand for different datasets, and different rows stand for different metrics. In each plot, the x -axis denotes the threshold and the y -axis denotes performance. For the first row, higher is better. For the last row, lower is better.

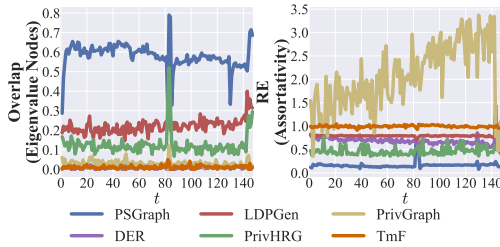


Figure 7: Performance of various methods on the As-733 dataset with different timestamps. For the left column, higher is better. For the right column, lower is better.

Kalman filter to predict non-sampled values, thereby correcting the noisy sampled values. Another direction involves the offline setting, where the server initially has a global view of all values and subsequently releases a streaming model that satisfies DP. In this context, Acs *et al.* [1] introduce an algorithm based on Discrete Fourier Transform.

w -event Privacy. To achieve a balance between privacy and utility at both event and user levels, w -event privacy is proposed for infinite streams, which protects every running window of at most w timestamps [6], [25], [32], [46], [51]. Bolot *et al.* [6] extend the binary tree mechanism for publishing perturbed answers on sliding window sum queries over infinite binary streams with fixed window sizes, introducing a relaxed privacy concept termed decayed privacy. Kellaris *et al.* [25] propose the notion of w -event DP and two novel privacy budget allocation schemes, where ϵ is divided among individual events to achieve the desired privacy level. Wang *et al.* [46] focus on the release of spatio-temporal trajectories and propose a framework called RescueDP, which incorporates a grouping strategy to partition the dimensions with similar statistics and changing trends to reduce the noise injection.

6.2. Differentially Private Graph Analysis

Differentially private graph analysis can perform a variety of statistical tasks on sensitive data. There are several works dedicated to specific downstream tasks [22], [24],

[38], [43], [49], [50], [53], including degree distribution, clustering coefficient, spectral graph analysis, *etc.* In particular, lipschitz extensions and exponential mechanism are employed to approximate the degree distribution for a sensitive graph in [38]. A constrained inference method is designed in [22] to publish the degree distribution. In [50], a divide-and-conquer approach is developed to obtain the clustering coefficient under DP. In addition, Wang *et al.* [49] propose two methods to calculate the eigen decomposition of the adjacency matrix while satisfying DP. Upadhyay *et al.* [43] aim to obtain a laplacian matrix in a DP manner.

6.3. Differentially Private Data Synthesis

There are some existing studies on differentially private data synthesis for other types of data, such as tabular data and trajectory data.

Tabular Data. There are three mainstream approaches for processing tabular data: graphical model-based, game-based, and deep generative model-based. The graphical model-based approaches focus on estimating a graphical model which approximates the distribution of the original dataset under DP [4], [10], [33], [57], [59]. The game-based approaches regard the dataset synthesis problem as a zero-sum game [19], [44]. Assuming that there are two players, *i.e.*, the data player and the query player, a no-regret learning algorithm for the data player is proposed to solve the game in [21]. Dual Query [19] switches the role of the data player and the query player. Deep generative model-based approaches initially train a deep generative model under DP and utilize the model to synthesize the dataset [3], [18], [58].

Trajectory Data. There are some works that investigate the synthesis of trajectory dataset under DP [8], [20], [23], [42], [45]. He *et al.* [23] design DPT, which takes into account the non-uniformity of true trajectories. AdaTrace proposed in [20] enforces deterministic constraints on the generated trajectories while satisfying DP, thereby enhancing the algorithm’s resilience against common threats. A method involving dynamic selection of first-order and second-order models is introduced in [45] to balance noise error and correlation error.

7. Conclusion

In this paper, we introduce PSGraph for publishing streaming graphs under DP. Our approach effectively preserves streaming graph information by extracting node details at the community level and applying essential post-processing techniques. Additionally, by leveraging temporal dynamics in the streaming data and aggregating relevant information across various timestamps, we efficiently conserve the privacy budget, resulting in synthetic graphs with superior utility compared to state-of-the-art methods. Extensive experiments on real-world datasets illustrate the superiority of PSGraph. We also conduct thorough ablation studies and parameter experiments to analyze the impact of various parts of PSGraph. The results indicate that the close integration of various modules in PSGraph can effectively capture the dynamic variations of streaming graphs.

References

- [1] G. Acs and C. Castelluccia. A Case Study: Privacy Preserving Release of Spatio-temporal Density in Paris. In *KDD*, 2014.
- [2] W. Aiello, F. Chung, and L. Lu. A Random Graph Model for Massive Graphs. In *STOC*, pages 171–180, 2000.
- [3] B. K. Beaulieu-Jones, Z. S. Wu, C. Williams, R. Lee, S. P. Bhavnani, J. B. Byrd, and C. S. Greene. Privacy-Preserving Generative Deep Neural Networks Support Clinical Data Sharing. *Circulation: Cardiovascular Quality and Outcomes*, 12(7):e005122, 2019.
- [4] V. Bindschaedler, R. Shokri, and C. A. Gunter. Plausible Deniability for Privacy-Preserving Data Synthesis. *Proceedings of the VLDB Endowment*, 10(5), 2017.
- [5] V. D. Blondel, J.-L. Guillaume, R. Lambiotte, and E. Lefebvre. Fast Unfolding of Communities in Large Networks. *Journal of Statistical Mechanics: Theory and Experiment*, 2008(10):P10008, 2008.
- [6] J. Bolot, N. Fawaz, S. Muthukrishnan, A. Nikolov, and N. Taft. Private Decayed Predicate Sums on Streams. In *ICDT*, pages 284–295, 2013.
- [7] Y. Cao, M. Yoshikawa, Y. Xiao, and L. Xiong. Quantifying Differential Privacy under Temporal Correlations. In *ICDE*, 2017.
- [8] R. Chen, G. Acs, and C. Castelluccia. Differentially Private Sequential Data Publication via Variable-Length N-Grams. In *CCS*, pages 638–649, 2012.
- [9] R. Chen, B. Fung, P. S. Yu, and B. C. Desai. Correlated Network Data Publication via Differential Privacy. *The VLDB Journal*, 23(4):653–676, 2014.
- [10] R. Chen, Q. Xiao, Y. Zhang, and J. Xu. Differentially Private High-Dimensional Data Publication via Sampling-Based Inference. In *KDD*, pages 129–138, 2015.
- [11] Y. Chen, A. Machanavajjhala, M. Hay, and G. Miklau. PeGaSus: Data-Adaptive Differentially Private Stream Processing. In *CCS*, page 1375–1388, 2017.
- [12] W. Dong, Q. Luo, and K. Yi. Continual Observation under User-level Differential Privacy. In *S&P*, pages 2190–2207, 2023.
- [13] C. Dwork, F. McSherry, K. Nissim, and A. Smith. Calibrating Noise to Sensitivity in Private Data Analysis. In *Theory of Cryptography Conference*, pages 265–284. Springer, 2006.
- [14] C. Dwork, M. Naor, T. Pitassi, and G. N. Rothblum. Differential Privacy under Continual Observation. In *STOC*, pages 715–724, 2010.
- [15] C. Dwork, A. Roth, et al. The Algorithmic Foundations of Differential Privacy. *Foundations and Trends® in Theoretical Computer Science*, 9(3–4):211–407, 2014.
- [16] Ú. Erlingsson, V. Feldman, I. Mironov, A. Raghunathan, K. Talwar, and A. Thakurta. Amplification by Shuffling: From Local to Central Differential Privacy via Anonymity. In *SODA*, 2019.
- [17] L. Fan and L. Xiong. An Adaptive Approach to Real-time Aggregate Monitoring with Differential Privacy. *TKDE*, 26(9):2094–2106, 2013.
- [18] L. Frigerio, A. S. d. Oliveira, L. Gomez, and P. Duverger. Differentially Private Generative Adversarial Networks for Time Series, Continuous, and Discrete Open Data. In *IFIP International Conference on ICT Systems Security and Privacy Protection*, 2019.
- [19] M. Gaboardi, E. J. G. Arias, J. Hsu, A. Roth, and Z. S. Wu. Dual Query: Practical Private Query Release for High Dimensional Data. In *ICML*, pages 1170–1178. PMLR, 2014.
- [20] M. E. Gursoy, L. Liu, S. Truex, L. Yu, and W. Wei. Utility-Aware Synthesis of Differentially Private and Attack-Resilient Location Traces. In *CCS*, pages 196–211, 2018.
- [21] M. Hardt, K. Ligett, and F. McSherry. A Simple and Practical Algorithm for Differentially Private Data Release. In *NeurIPS*, 2012.
- [22] M. Hay, C. Li, G. Miklau, and D. Jensen. Accurate Estimation of the Degree Distribution of Private Networks. In *ICDM*, 2009.
- [23] X. He, G. Cormode, A. Machanavajjhala, C. M. Procopiuc, and D. Srivastava. DPT: Differentially Private Trajectory Synthesis Using Hierarchical Reference Systems. *PVLDB*, 8(11):1154–1165, 2015.
- [24] S. P. Kasiviswanathan, K. Nissim, S. Raskhodnikova, and A. Smith. Analyzing Graphs with Node Differential Privacy. In *Theory of Cryptography Conference*, pages 457–476. Springer, 2013.
- [25] G. Kellaris, S. Papadopoulos, X. Xiao, and D. Papadias. Differentially Private Event Sequences over Infinite Streams. *PVLDB*, 2014.
- [26] T. Khafaei, A. Tavakoli Taraghi, M. Hosseinzadeh, and A. Rezaee. Tracing Temporal Communities and Event Prediction in Dynamic Social Networks. *Social Network Analysis and Mining*, 9:1–11, 2019.
- [27] A. Khrabrov and G. Cybenko. Discovering Influence in Communication Networks Using Dynamic Graph Analysis. In *2010 IEEE Second International Conference on Social Computing*, pages 288–294, 2010.
- [28] S. Kumar, W. L. Hamilton, J. Leskovec, and D. Jurafsky. Community Interaction and Conflict on the Web. In *WWW*, pages 933–943, 2018.
- [29] J. Leskovec, J. Kleinberg, and C. Faloutsos. Graphs Over Time: Densification Laws, Shrinking Diameters and Possible Explanations. In *KDD*, pages 177–187, 2005.
- [30] J. Leskovec, J. Kleinberg, and C. Faloutsos. Graph Evolution: Densification and Shrinking Diameters. *TKDD*, 2007.
- [31] H. Li, L. Xiong, X. Jiang, and J. Liu. Differentially Private Histogram Publication for Dynamic Datasets: An Adaptive Sampling Approach. In *CIKM*, pages 1001–1010, 2015.
- [32] Z. Ma, T. Zhang, X. Liu, X. Li, and K. Ren. Real-time Privacy-preserving Data Release over Vehicle Trajectory. *IEEE Transactions on Vehicular Technology*, 68(8):8091–8102, 2019.
- [33] R. McKenna, D. Sheldon, and G. Miklau. Graphical-Model Based Estimation and Inference for Differential Privacy. In *International Conference on Machine Learning*, pages 4435–4444. PMLR, 2019.
- [34] F. McSherry and K. Talwar. Mechanism Design via Differential Privacy. In *FOCS*, pages 94–103, 2007.
- [35] H. H. Nguyen, A. Imine, and M. Rusinowitch. Differentially Private Publication of Social Graphs at Linear Cost. In *ASONAM*, 2015.
- [36] V. Perrier, H. J. Asghar, and D. Kaafar. Private Continual Release of Real-valued Data Streams. In *NDSS*, 2019.
- [37] Z. Qin, T. Yu, Y. Yang, I. Khalil, X. Xiao, and K. Ren. Generating Synthetic Decentralized Social Graphs with Local Differential Privacy. In *CCS*, pages 425–438, 2017.
- [38] S. Raskhodnikova and A. Smith. Lipschitz Extensions for Node-Private Graph Statistics and the Generalized Exponential Mechanism. In *FOCS*, pages 495–504, 2016.

- [39] R. A. Rossi, B. Gallagher, J. Neville, and K. Henderson. Modeling Dynamic Behavior in Large Evolving Graphs. In *WSDM*, pages 667–676, 2013.
- [40] A. Sala, X. Zhao, C. Wilson, H. Zheng, and B. Y. Zhao. Sharing Graphs Using Differentially Private Graph Models. In *SIGCOMM*, pages 81–98, 2011.
- [41] V. Sekara, A. Stopczynski, and S. Lehmann. Fundamental Structures of Dynamic Social Networks. *PNAS*, 113(36):9977–9982, 2016.
- [42] X. Sun, Q. Ye, H. Hu, Y. Wang, K. Huang, T. Wo, and J. Xu. Synthesizing Realistic Trajectory Data with Differential Privacy. *IEEE Transactions on Intelligent Transportation Systems*, 2023.
- [43] J. Upadhyay, S. Upadhyay, and R. Arora. Differentially Private analysis on Graph Streams. In *International Conference on Artificial Intelligence and Statistics*, pages 1171–1179. PMLR, 2021.
- [44] G. Vietri, G. Tian, M. Bun, T. Steinke, and S. Wu. New Oracle-Efficient Algorithms for Private Synthetic Data Release. In *ICML*, pages 9765–9774. PMLR, 2020.
- [45] H. Wang, Z. Zhang, T. Wang, S. He, M. Backes, J. Chen, and Y. Zhang. PrivTrace: Differentially Private Trajectory Synthesis by Adaptive Markov Model. In *USENIX Security Symposium*, 2023.
- [46] Q. Wang, Y. Zhang, X. Lu, Z. Wang, Z. Qin, and K. Ren. Real-time and Spatio-temporal Crowd-sourced Social Network Data Publishing with Differential Privacy. *TDSC*, 15(4):591–606, 2016.
- [47] T. Wang, J. Q. Chen, Z. Zhang, D. Su, Y. Cheng, Z. Li, N. Li, and S. Jha. Continuous Release of Data Streams under both Centralized and Local Differential Privacy. In *CCS*, pages 1237–1253, 2021.
- [48] T. Wang, M. Lopuhaä-Zwakenberg, Z. Li, B. Skoric, and N. Li. Locally Differentially Private Frequency Estimation with Consistency. In *NDSS*, 2020.
- [49] Y. Wang, X. Wu, and L. Wu. Differential Privacy Preserving Spectral Graph Analysis. In *PAKDD*, pages 329–340, 2013.
- [50] Y. Wang, X. Wu, J. Zhu, and Y. Xiang. On Learning Cluster Coefficient of Private Networks. *Social Network Analysis and Mining*, 3(4):925–938, 2013.
- [51] Z. Wang, X. Pang, Y. Chen, H. Shao, Q. Wang, L. Wu, H. Chen, and H. Qi. Privacy-preserving Crowd-sourced Statistical Data Publishing with An Untrusted Server. *IEEE Transactions on Mobile Computing*, 18(6):1356–1367, 2018.
- [52] Q. Xiao, R. Chen, and K.-L. Tan. Differentially Private Network Data Release via Structural Inference. In *KDD*, pages 911–920, 2014.
- [53] Q. Ye, H. Hu, M. H. Au, X. Meng, and X. Xiao. Towards Locally Differentially Private Generic Graph Metric Estimation. In *ICDE*, pages 1922–1925, 2020.
- [54] F. Yin, Y. Liu, Z. Shen, L. Chen, S. Shang, and P. Han. Next POI Recommendation with Dynamic Graph and Explicit Dependency. In *AAAI*, pages 4827–4834, 2023.
- [55] W. Yu, C. C. Aggarwal, S. Ma, and H. Wang. On Anomalous Hotspot Discovery in Graph Streams. In *ICDM*, pages 1271–1276, 2013.
- [56] Q. Yuan, Z. Zhang, L. Du, M. Chen, P. Cheng, and M. Sun. PrivGraph: Differentially Private Graph Data Publication by Exploiting Community Information. In *USENIX Security Symposium*, 2023.
- [57] J. Zhang, G. Cormode, C. M. Procopiuc, D. Srivastava, and X. Xiao. PrivBayes: Private Data Release via Bayesian Networks. *ACM Transactions on Database Systems (TODS)*, 42(4):1–41, 2017.
- [58] X. Zhang, S. Ji, and T. Wang. Differentially Private Releasing via Deep Generative Model. *CoRR*, abs/1801.01594, 2018.
- [59] Z. Zhang, T. Wang, J. Honorio, N. Li, M. Backes, S. He, J. Chen, and Y. Zhang. PrivSyn: Differentially Private Data Synthesis. In *USENIX Security Symposium*, 2021.
- [60] T. Zhu, G. Li, W. Zhou, and S. Y. Philip. Differentially Private Data Publishing and Analysis: A Survey. *TKDE*, 29(8):1619–1638, 2017.

Appendix

1. Overall Workflow of PSGraph

Algorithm 4 describes the workflow of PSGraph. Based on the total privacy budget ε and window size w , we can obtain the privacy budget ε_s^t at each timestamp by average allocation. The budget allocation for a single timestamp can be adjusted according to the graph. Initially, we determine the privacy budget ε_e^t allocated for perturbing the total number of edges. As the total number of edges is usually large and the sensitivity is 1, we limit this portion of the privacy budget to a maximum of 0.01. Furthermore, the remaining privacy budget ε_r^t is computed (**Line 1**). At each timestamp, the perturbed number of edges m_{pert}^t can be obtained (**Line 2**). If $t = 1$, the privacy budget ε_c^t is allocated for community partitioning, and ε_i^t is allocated for information perturbation (**Line 3–Line 6**). For subsequent timestamps, the information from the last graph can aid in community division and information perturbation at t . The difference δ_e in perturbed edges between the adjacent timestamps can be calculated (**Line 8**). If δ_e exceeds the number of nodes, indicating significant changes in the two graphs, the privacy budget $\varepsilon_c^t = 0.5\varepsilon_r^t$ is allocated for community re-partitioning (**Line 9–Line 11**). Conversely, if the difference is small, the previous community partition can be retained, with $\varepsilon_i^t = \varepsilon_r^t$ allocated for information perturbation (**Line 12–Line 14**). Once the community structure is determined, **Algorithm 2** is employed to perturb true information (**Line 15**). Finally, the entire graph is reconstructed using **Algorithm 3**.

2. Proof of Theorem 1

PSGraph consists of three phases: Community determination, information perturbation, and graph reconstruction. Next, we show that PSGraph satisfies w -event ε -edge DP, where $\varepsilon = w \cdot \varepsilon_s$ and $\varepsilon_s = \varepsilon_e^t + \varepsilon_c^t + \varepsilon_i^t$.

Proof 1: Community determination satisfies $(\varepsilon_e^t + \varepsilon_c^t)$ -edge DP.

Proof. In the community determination, PSGraph first perturb the true number of edge based on Laplace mechanism, which can provide rigorous differential privacy guarantee. The privacy budget consumed in this step is ε_e^t . Then, the difference in the number of perturbed edges between the current timestamp and the last timestamp determines whether to retain the previous community or re-partition. If the communities from last timestamp is retained, it does not consume any privacy budget, *i.e.*, $\varepsilon_c^t = 0$. Conversely, if the community needs to be re-partition, the Laplace mechanism is adopted to perturb the weights of supernodes, while exponential mechanism is utilized to determine the nodes’ final community, both of which meet the requirements of DP. The detailed proof of the re-partition is in Appendix A of [56]. Therefore, the community division step satisfies ε_c^t -edge DP. Further, the community determination satisfies $(\varepsilon_e^t + \varepsilon_c^t)$ -edge DP based on sequential composition of DP. \square

Algorithm 4: PSGraph

Input: Current timestamp t , original graph G_t , total privacy budget ε , window size w , privacy budget at current timestamp $\varepsilon_s^t = \varepsilon/w$, privacy budget for edge perturbation ε_e^t , privacy budget for community division ε_c^t , privacy budget for information perturbation ε_i^t ,

Output: Synthetic graph G_s^t

```
1  $\varepsilon_e^t = \min(0.01, 0.5\varepsilon_s^t)$ ,  $\varepsilon_r^t = \varepsilon_s^t - \varepsilon_e^t$ 
2  $m_{pert}^t \leftarrow m^t + \text{Laplace}(\varepsilon_e^t, \Delta f_e)$ 
3 if  $t = 1$  then
4    $\varepsilon_c^t = 0.5\varepsilon_r^t$ ,  $\varepsilon_i^t = \varepsilon_r^t - \varepsilon_c^t = 0.5\varepsilon_r^t$ 
5   Obtain the community division  $\mathbb{C}_D$ 
   using Algorithm 1 with  $\varepsilon_c^t$ 
6   Perturb the true information using Algorithm 2
   and  $\mathbb{C}_D$  with  $\varepsilon_i^t$ 
7 else
8    $\delta_e = |m_{pert}^t - m_{pert}^{t-1}|$ 
9   if  $\delta_e > N^t$  then
10     $\varepsilon_c^t = 0.5\varepsilon_r^t$ ,  $\varepsilon_i^t = \varepsilon_r^t - \varepsilon_c^t = 0.5\varepsilon_r^t$ 
11    Obtain  $\mathbb{C}_D$  by re-partitioning the community
    using Algorithm 1 with  $\varepsilon_c^t$ 
12  else
13     $\varepsilon_c^t = 0$ ,  $\varepsilon_i^t = \varepsilon_r^t$ 
14     $\mathbb{C}_D \leftarrow \mathbb{C}_L$ 
15    Perturb the true information using Algorithm 2
    and  $\mathbb{C}_D$  with  $\varepsilon_i^t$ 
16 Reconstruct the graph using Algorithm 3
```

Proof 2: Information perturbation satisfies ε_i^t -edge DP.

Proof. In the information perturbation phase, the degree information within and outside the community, and the edge count between various communities are injected Laplace noise, respectively. Note that both the degree information outside the community and the edge count between communities require access to the edges of inter-community, thus their privacy budget allocation needs to follow sequential property of DP. On the other hand, the degree information within the community needs to visit the edges of intra-community, which does not intersect with the above two. Then, the degree information of intra-community can be perturbed by the same privacy budget based on the parallel composition. Therefore, the information perturbation satisfies ε_i^t -edge DP. \square

Overall Privacy Budget. According to the above proofs, in the first phase, community determination satisfies $(\varepsilon_e^t + \varepsilon_c^t)$ -edge DP. The information perturbation phase satisfies ε_i^t -edge DP. In graph reconstruction, PSGraph processes the perturbed data without consuming privacy budget. In accordance with sequential composition, PSGraph satisfies ε_s -edge DP at a single timestamp. Since the privacy budget at each timestamp is the same, PSGraph satisfies w -event ε -edge DP for any w timestamps.

TABLE 4: Comparison of running time (measured by seconds).

Methods	Datasets			
	As-733	As-caida	Cit-HepPh	Reddit
TmF	70.84	481.49	16.88	19.88
PrivGraph	310.89	1998.91	46.93	101.60
DER	8772.87	48223.78	3705.31	5140.13
PrivHRG	35281.87	270312.32	4328.67	10091.21
LDPGen	512.87	1256.19	101.42	284.64
PSGraph	678.94	1242.34	35.81	104.58

3. Complexity Analysis

In the section, we analyze the computational complexity of PSGraph, and quantitatively compare its running time and memory consumption with other methods.

Computational Complexity. We adopt m to represent the number of edges and n to represent the number of nodes. For the time complexity of PSGraph, in the first phase, if there are significant variations between adjacent two graphs, it is essential to re-partition the community, which requires the complexity of $\mathcal{O}(n^2)$. In the information perturbation phase, the degree information of nodes and the edge count between various communities are perturbed, thus the corresponding time complexity is $\mathcal{O}(n + k^2)$, where k is the number of communities. The time complexity of the graph reconstruction phase is similar to that of the second phase. Above all, we can obtain $\mathcal{O}(n^2) + \mathcal{O}(n) + \mathcal{O}(k^2) = \mathcal{O}(n^2 + n + k^2) < \mathcal{O}(n^2)$, thus the total time complexity is $\mathcal{O}(n^2)$. Actually, community re-partitioning is not necessary at each timestamp, so the overall runtime is acceptable. For the space complexity of PSGraph, it requires to store the edge information from all nodes to various communities, we can obtain $\mathcal{O}(nk) < \mathcal{O}(n^2)$, where k is the number of communities. Therefore, the space complexity is $\mathcal{O}(n^2)$. In addition, the time and space complexity of other methods has already been analyzed in [56], and we omit it here.

Empirical Evaluation. Table 4 and Table 5 show the running time and the memory consumption for all methods on the four datasets (see their details in Table 2). The running time in Table 4 illustrates that the performance of TmF is the best because it perturbs the cells in a linear time. The running time of PSGraph, PrivGraph and LDPGen are longer than TmF due to community division. However, community partitioning is fast, and it's not always necessary for PSGraph. Therefore, PSGraph still performs better compared to most methods. PrivHRG and DER take much more time than other methods. PrivHRG spends a lot of time to sample an HRG, and DER consumes abundant time dividing the adjacency matrix into small pieces at each timestamp.

Table 5 illustrates the memory consumption. We can see that DER occupies the most memory. This is because DER requires maintaining a count matrix during data processing. PSGraph also necessitates a substantial amount of memory to store information related to nodes and communities. Overall, this level of resource usage is acceptable.

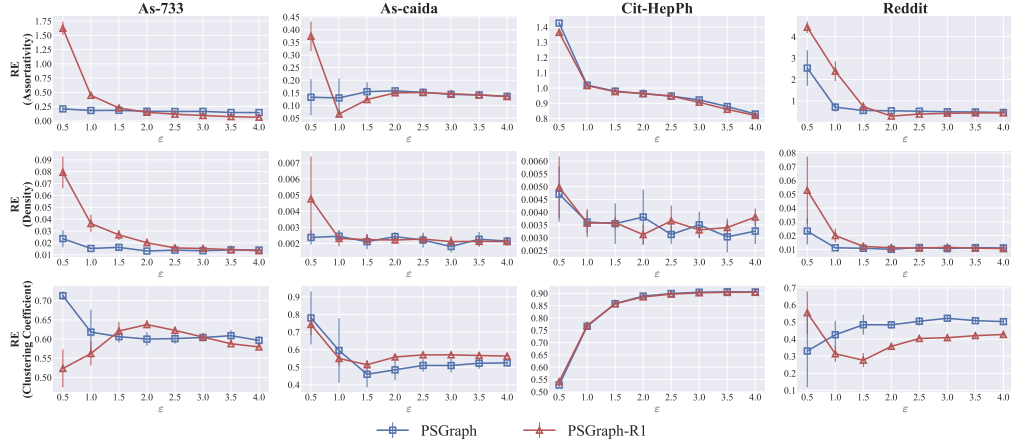


Figure 8: [Lower is better] Comparison of PSGraph and PSGraph-R1. The columns represent the used datasets, and the rows stand for different metrics. In each plot, the x -axis denotes the privacy budget ϵ and the y -axis denotes performance.

TABLE 5: Comparison of memory consumption (measured by Megabytes).

Methods	Datasets			
	As-733	As-caida	Cit-HepPh	Reddit
TmF	262.26	580.06	127.64	311.56
PrivGraph	267.47	610.24	159.23	361.23
DER	505.12	7340.03	382.29	1120.26
PrivHRG	282.15	694.23	173.21	372.19
LDPGen	318.95	1604.09	183.07	455.86
PSGraph	385.09	2367.49	295.12	767.32

4. Ablation Study

4.1. Impact of the Community Judgment. Figure 8 illustrates the comparison result of PSGraph and PSGraph-R1 across three metrics. Regarding the assortativity coefficient, PSGraph maintains consistently low errors on As-733 and As-caida datasets. In contrast, PSGraph-R1 exhibits significant errors when the privacy budget is limited, due to the substantial privacy budget required for each community re-partitioning. This disparity is particularly pronounced under low privacy budget conditions. For Cit-HepPh, where temporal dynamics are less clear, PSGraph and PSGraph-R1 perform similarly, reflecting the dataset’s characteristics. PSGraph also demonstrates advantages in density preservation, underscoring the significance of the community judgment mechanism. While PSGraph-R1 occasionally shows improved performance in clustering coefficients, attributed to the beneficial effects of periodic community re-partitioning on node clustering, PSGraph remains competitive performance. These results highlight the robust performance of PSGraph across various datasets with differing levels of temporal dynamics and emphasize the critical role of community judgment in achieving effective privacy-preserving graph synthesis.

4.2. Impact of Various Components. Figure 9 illustrates the impact of various components on three metrics. Ablation2, which only incorporates information fusion, exhibits poorer performance on these metrics. This is primarily because the inclusion of information from previous moments may disrupt the total counts of edges and triangles in the current state. Thus, the REs of Ablation2 in density and clustering coefficients are higher compared to Ablation1 without information fusion, especially when the privacy budget is high. Ablation3 and Ablation4, incorporating post-processing, demonstrate better performance in density and clustering coefficient metrics than Ablation1 and Ablation2. This improvement arises from the constraints imposed on total edge count and node degree information by post-processing. For the assortativity coefficient, when ϵ is small, Ablation3 without information fusion is less effective than Ablation4 with information fusion. As ϵ increases, the disturbance at the current timestamp decreases, leading to a notable improvement in the effectiveness of Ablation3.

5. Parameter Variation

5.1. Impact of Window Size. Figure 10 illustrates the results for three metrics across different w when $\epsilon = 2.5$. Overall, PSGraph demonstrates competitive performance across most scenarios. Regarding the assortativity coefficient, PSGraph outperforms other methods on the first two datasets but shows increasing REs on the latter two datasets as w increases. This is mainly due to pronounced variations in the Cit-HepPh dataset where the dynamic mechanism of PSGraph has limited impact under small privacy budgets. Additionally, the assortativity coefficient of Reddit is low, and the noise in degree information extracted by PSGraph with large w is significant, resulting in high REs. For density, both PSGraph and TmF exhibit performance close to 0, while other methods show significant increases with w , underscoring the importance of the post-processing step for PSGraph. In terms of clustering coefficient, PSGraph and LDPGen perform better across different w values compared to other methods. However, the trend in

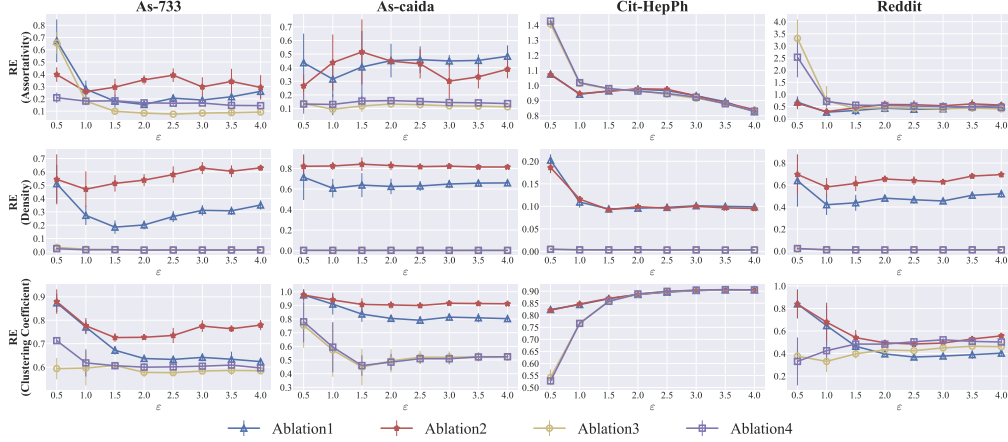


Figure 9: [Lower is better] Effectiveness of various components. Ablation1 represents PSGraph without information fusion and post-processing, Ablation2 represents PSGraph without post-processing, Ablation3 represents PSGraph without information fusion, and Ablation4 represents PSGraph. The columns represent the datasets, and the rows stand for different metrics. In each plot, the x -axis denotes the privacy budget ϵ and the y -axis denotes performance.

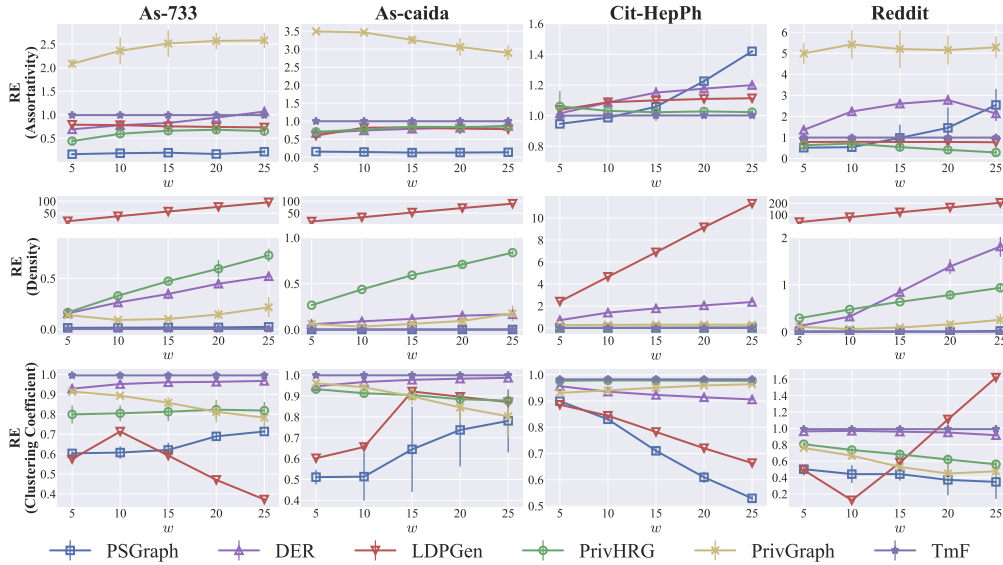


Figure 10: [Lower is better] Impact of window size. Different columns stand for different datasets, and different rows stand for different metrics. In each plot, the x -axis denotes the number of window size w and the y -axis denotes performance.

clustering coefficient varies across datasets as w increases, influenced by the varying clustering situations. For instance, for the Cit-HepPh dataset with high clustering, PSGraph and LDPGen tend to produce more triangles as w increases, which in turn leads to smaller REs.

5.2. Impact of Threshold. Figure 11 illustrates the performance of three metrics across various thresholds. Similar to Figure 6, the choice of threshold is influenced by the dataset, privacy budget, and metric type. PSGraph achieves favorable results with KL divergence at larger thresholds primarily because such thresholds effectively preserve similar information across different timestamps, thereby enhancing accuracy in degree distribution. For density, PSGraph ex-

hibits larger errors on Cit-HepPh at larger thresholds due to drastic inherent time variations. For clustering coefficients across most datasets, PSGraph shows smaller errors at smaller thresholds, which contrasts with the trend observed in KL divergence. Consequently, there is no universally optimal threshold that satisfies all configurations. When the threshold is set to the number of nodes, PSGraph can achieve competitive results across varied settings.

6. Ethical Use of Data

We strictly followed ethical guidelines by using publicly available, open-source datasets under licenses permitting research and educational use.

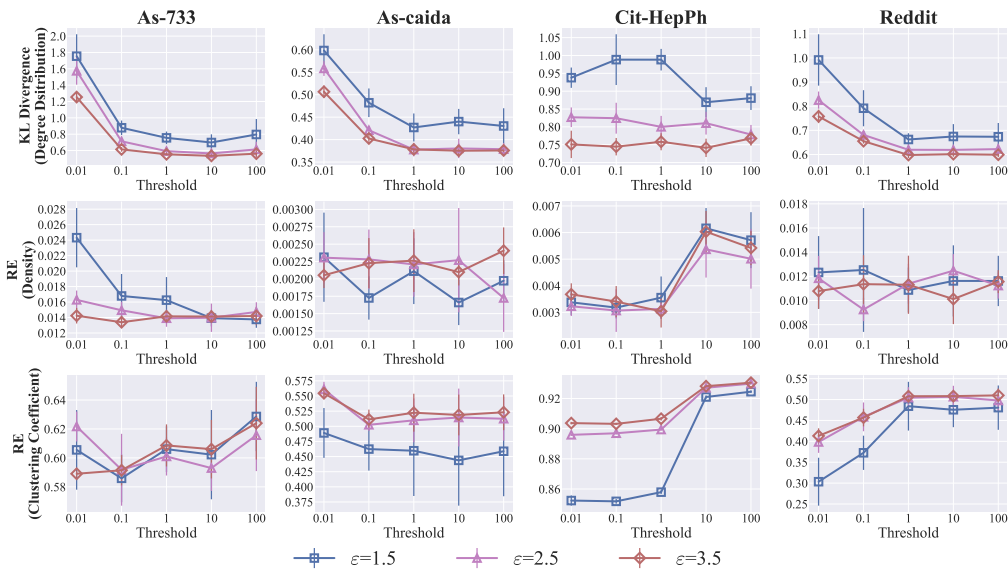


Figure 11: [Lower is better] Impact of threshold. Different columns stand for different datasets, and different rows stand for different metrics. In each plot, the x -axis denotes the threshold and the y -axis denotes performance.